

Energy dissipation of electron solitons in a quantum well

S. Bednarek and B. Szafran

Faculty of Physics and Applied Computer Science, AGH University of Science and Technology, PL-30059 Kraków, Poland

(Received 5 January 2006; revised manuscript received 3 February 2006; published 18 April 2006)

A linear response theory is provided for the dynamic interaction effects of an electron soliton confined in semiconductor quantum well with a conducting surface or a two-dimensional electron gas. It is shown that the soliton-electron-gas effective potential contains a dissipative component resisting against changes of the soliton charge density. Due to the energy dissipation moving solitons are stopped and the nonstationary excitations of the wave packet relax to the standing ground state.

DOI: [10.1103/PhysRevB.73.155318](https://doi.org/10.1103/PhysRevB.73.155318)

PACS number(s): 73.63.Hs, 05.45.Yv, 05.60.Gg

I. INTRODUCTION

An electron placed close to a metal plate induces a charge redistribution in the conductor resulting in the formation of an induced surface charge attracting the electron. In electrostatic quantum dots the interaction of the confined charge and the charge induced on metal gates significantly lowers the energies of the confined electrons.¹⁻³ Recently,⁴ we demonstrated that an electron confined in a semiconductor quantum well becomes self-trapped by the potential of the charge it induces on an infinite conducting plate or alternatively in a second semiconductor quantum well containing a two-dimensional electron gas (2DEG). The self-interaction laterally localizes the electron forming a stable nearly Gaussian wave packet of a finite size.⁴ The packet can move parallel to the surface of the conductor without changing its shape behaving like a soliton. Since the potential forming the wave packet is due to the induced charge we will refer to it as an *inducton*. The soliton exhibits semiclassical scattering properties, in particular, a binary 0/100% probability of passing through obstacles.⁴ Therefore, the inducton is likely to find applications in spintronics, single-electron devices, and in the construction of logical gates for a quantum computer.

In Ref. 4 we discussed the basic properties of the inducton under the assumption of an ideal conductor. We showed that the static ($\omega=0$) response of the medium does not qualitatively change the results of the image charge approach, although it reduces the interaction quantitatively weakening the self-focusing effect. In the present paper we study the dynamics ($\omega \neq 0$) of the interaction between the inducton and the 2DEG in a realistic system. We find that 2DEG dissipates the inducton energy, which introduces important new properties of the electron soliton. A similar energy dissipation mechanism was considered for the image charge states at metal and/or dielectric interfaces.⁵ It was demonstrated⁵ that the dynamical response of the electron gas on the external perturbation leads to finite electron lifetimes in the Rydberg image-potential states delocalized parallel to the interface. The dynamical response of the electron gas to the fast ion in context of the plasmon excitations was discussed.⁶ For the electron solitons we are interested in the opposite—low velocity limit of the response. Recently, the time evolution of the screening process for a charge suddenly created in a two-dimensional electron gas has been calculated.⁷ Here, we con-

sider the time evolution of the entire quantum system of the soliton Coulomb coupled to the electron gas. In particular, we describe the effect of the soliton charge perturbing the electron gas and the response of the gas influencing the soliton wave function.

II. IDEAL CONDUCTOR MODEL

We consider an electron in a semiconductor quantum well near a parallel, infinite conducting plane. Under the assumption of the ideal conductor the interaction energy of the charge of density ρ^{el} with the induced charge ρ^i can be evaluated by the method of images

$$W = \frac{1}{2} \int d^6r \rho^{el}(\mathbf{r}) V^c(\mathbf{r} - \mathbf{r}') \rho^i(\mathbf{r}'), \quad (1)$$

where $V^c = \kappa/r$, $\kappa = e^2/4\pi\epsilon\epsilon_0$, and $\rho^i(x, y, z) = -\rho^{el}(x, y, -z)$ (we take $z=0$ at the conducting plane). The $\frac{1}{2}$ factor in front of the integral in Eq. (1) is due to the self-interaction character of the effect. The sum of the electron-image interaction energy and the expected value of the kinetic energy operator T gives the total energy of the system $E^{tot} = \langle \psi | T | \psi \rangle + W$. The eigenequation for the electronic wave function $\psi(\mathbf{r})$ is obtained requiring that the variation of E^{tot} with respect to $\psi^*(\mathbf{r})$ vanishes, $(H - E)\psi(\mathbf{r}) = 0$. The obtained single-electron Hamiltonian $H = T + U$ is the sum of the kinetic energy operator T and the potential energy of the electron in the electrostatic field of the image charge potential

$$U(\mathbf{r}) = |e| \int d^3r' V^c(\mathbf{r} - \mathbf{r}') \rho^i(\mathbf{r}'). \quad (2)$$

Note, that, due to the square dependence of the interaction energy (1) on ψ^* the $\frac{1}{2}$ factor before the integral vanishes. Similarly, the eigenvalue $E = E^{tot} + W$ is not identical to the total energy E^{tot} , but contains a double value of the interaction energy W . It is a characteristic feature of single-electron Hamiltonian eigenvalues in the mean field approximation.

In the following we will refer to E —the eigenvalue of H —as the single-electron energy. In physical processes, the total and the single-electron energies play different roles. The time evolution of a quantum state is found from the Schrödinger equation with the single-electron Hamiltonian H

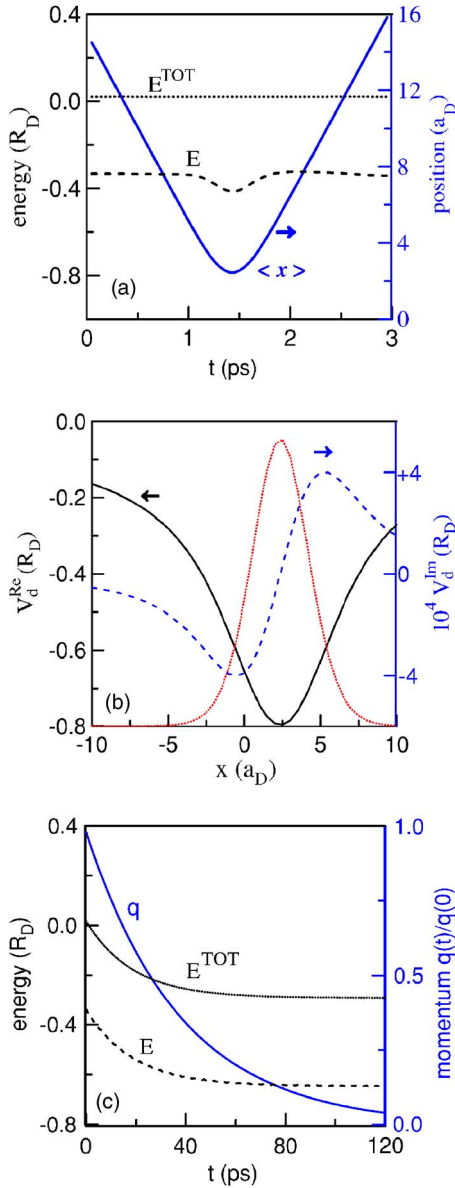


FIG. 1. (Color online) (a) Single-electron (dashed curve) and total (dotted curve) energies (left axis) for the inductor scattering from a high potential barrier in the ideal conductor approximation. The position of the inductor center is plotted with the solid line and is referred to the right axis. (b) Potentials stemming from the real (solid line—left axis) and the imaginary (dashed line—right axis) part of the Fourier transform of the induced potential for the inductor charge density (plotted with the dotted line) moving right with momentum $q=0.1k_F$ (see text). (c) Single-electron (dashed curve) and total (dotted curve) energies (left axis) for the free inductor dissipating its kinetic energy via interaction with the electron gas. The solid line shows the momentum (right axis).

including the potential energy $U(\mathbf{r})$. Therefore, in the energy eigenstates the spatial wave function is multiplied by the time-dependent factor with the single-electron energy.⁴ However, in the elastic scattering processes it is the total energy that is conserved, and not the single-electron energy. Figure 1(a) illustrates the reflection of the moving inductor from a high potential barrier. The solid line shows the expectation

value of the position of the moving wave packet. Initially the inductor moves down the axis with a constant velocity, which corresponds to the straight part of the curve. The barrier set at the origin reflects the wave packet. The solid line does not reach the origin but it turns back upward, passing to another straight line. When the velocity is constant so are the total and the single-electron energies. The charge density of the wave packet is temporarily increased during the reflection near the barrier. In consequence the absolute value of the interaction of the electron wave packet with the induced charge is also increased. This in turn leads to a dip in the single-electron energy (the dashed line). The total energy (dotted line) is constant during the entire process.

III. RESPONSE OF THE TWO-DIMENSIONAL ELECTRON GAS

The behavior of the system presented in Fig. 1(a) is a result obtained with the assumption of the ideal conductor, which immediately screens the external potential by formation of a proper surface charge. Let us calculate the induced potential for the dynamic response of the conducting medium on the electron charge localized in the quantum well. Similarly as in Ref. 4 for the illustration of the quantum effects appearing at the conductor surface we use a two-dimensional model of the electron gas and apply the linear response approximation. The adopted model is presented in Fig. 1(a) of Ref. 4. It consists of two parallel quantum wells QW_0 ($z=0$) and QW_d ($z=d$), separated by the tunnel barrier of width d (in the following we will distinguish all the physical quantities by a subscript “0” for QW_0 and “ d ” for QW_d). For the sake of simplicity we assume that the quantum wells are strictly two-dimensional and described by the pair of (x, y) coordinates. The bottom of the deeper quantum well QW_0 is below the Fermi level deep enough for the 2DEG formation. The quantum well QW_d is shallower and its bottom lies above the Fermi level. We place a single electron in the shallow quantum well QW_d . Moreover, we assume that the quantum wells and the barrier are made of similar materials, so that we can adopt the same effective masses and dielectric constants. The present model allows for a simpler solution than for the electron gas in metal and the model structure for which the calculations are performed can also be realized experimentally. We expect that the obtained results are qualitatively correct also for the metal plate. Let us note that the discussed situation differs from a typical⁸ problem of the external potential screening inside the electron gas, since the electron—the source of the perturbing potential—lies outside the perturbed medium. Moreover, we look for the distribution of the induced potential outside the medium.

Let us assume that the single electron in QW_d is in the state described by a wave function $\psi_d(\mathbf{r}, t)$. Its charge density $\rho^e(\mathbf{r}, t) = |\psi_d(\mathbf{r}, t)|^2$ is a source of the electric field, with the potential that in the three-dimensional space has the form

$$V^e(\mathbf{r}, z, t) = -|e|\kappa \int d^2r' \frac{\rho_d^e(\mathbf{r}', t)}{\sqrt{(\mathbf{r} - \mathbf{r}')^2 + (z - d)^2}}. \quad (3)$$

This potential is an external perturbation for the 2DEG in QW_0 . In the following we will need the Fourier transform of

this potential at $z=0$: $V_0^{ext}(\mathbf{r}, t) = V^{el}(\mathbf{r}, 0, t)$. It is a product $V_0^{ext}(\mathbf{k}, \omega) = \rho_d^{el}(\mathbf{k}, \omega) V_d^c(k)$ of the Fourier transform of the electron charge and the transform of the Coulomb potential

$$V_d^c(k) = \kappa \int d^2r \frac{e^{i\mathbf{k}\cdot\mathbf{r}}}{\sqrt{d^2 + r^2}} = \kappa \frac{2\pi e^{-kd}}{k}. \quad (4)$$

The perturbing potential V_0^{ext} results in the induced potential V_0^{ind} which is the response of the medium. Their sum yields the total potential $V_0^{tot} = V_0^{ext} + V_0^{ind}$. We will calculate the induced potential using the linear response method. In this approximation the Fourier transform of the induced potential is proportional to the Fourier transform of the total potential,

$$V^{ind}(\mathbf{k}, \omega) = V^{tot}(\mathbf{k}, \omega) V_0^c(k) \chi_0(\mathbf{k}, \omega), \quad (5)$$

where $V_0^c(k)$ is the two-dimensional Fourier transform of the Coulomb potential $V_0^c(\mathbf{k}) = \kappa 2\pi/k$, and the response function $\chi_0(\mathbf{k}, \omega)$ can be approximated by the Lindhard formula for the 2DEG

$$\chi_0(\mathbf{k}, \omega) = \frac{2}{(2\pi)^2} \int d^2q \frac{f(E_{\mathbf{q}+\mathbf{k}}) - f(E_{\mathbf{q}})}{E_{\mathbf{q}+\mathbf{k}} - E_{\mathbf{q}} - \hbar\omega + i\hbar\alpha}. \quad (6)$$

The response function is calculated assuming a parabolic dispersion relation for E_k with the electron effective mass, and the Fermi-Dirac distribution is taken as a step function ($T=0$ K). In a general case, the response function is given by a relatively complex⁸ function of k , the Fermi wave vector k_F , and the Fermi energy E_F and can only be applied in numerical calculations. In the following analytical expression we consider the high Fermi energy limit, i.e., $k \ll k_F$, $\hbar\omega \ll E_F$. In this limit the response function takes the form

$$\chi_0(\mathbf{k}, \omega) = -\frac{m}{\pi\hbar^2} \left(1 + i \frac{m\omega}{\hbar^2 k k_F} \right). \quad (7)$$

This function differs from the one calculated in Ref. 4 by the imaginary term proportional to ω , which vanishes for the static potential. Finally, we obtain the Fourier transform of the induced potential in QW_d as

$$V_d^{ind}(k, \omega) = -\frac{2\pi\kappa e^{-2kd}}{k} \rho_d^{el}(\mathbf{k}, \omega) \times \frac{\left(\frac{\hbar^2 k}{2m\kappa} + 1 + \frac{m^2 \omega^2}{\hbar^2 k^2 k_F^2} + i \frac{\hbar\omega}{2\kappa k_F} \right)}{\left(\frac{\hbar^2 k}{2m\kappa} + 1 \right)^2 + \left(\frac{m\omega}{\hbar k k_F} \right)^2}. \quad (8)$$

For a nonzero inducton velocity an imaginary part of the induced potential appears in the wave vector space. It is inversely proportional to the Fermi wave vector in the 2DEG. In the considered limit of high k_F the imaginary contribution is small, but we account for it since it leads to a new effect. Conversely, we neglect the real components inversely proportional to k_F^2 . Furthermore we neglect the term proportional to k in the denominator of Eq. (8)

$$V_d^{ind}(\mathbf{k}, \omega) = -\frac{2\pi\kappa e^{-2kd}}{k} \left(1 + \frac{i\hbar\omega}{2\kappa k_F} \right) \rho_d^{el}(\mathbf{k}, \omega), \quad (9)$$

which will allow us to express the induced potential in the real space in terms of the image charge potential (2) (see below). The real and imaginary parts of the induced potential (9) transformed to the real space give the potential components of different physical meaning $V^{ind}(\mathbf{r}, t) = V_d^{Re}(\mathbf{r}, t) + V_d^{Im}(\mathbf{r}, t)$, where

$$V_d^{Re}(\mathbf{r}, t) = U(\mathbf{r}, t) = -|e|\kappa \int d^2r' \frac{\rho_d^{el}(\mathbf{r}', t)}{\sqrt{(\mathbf{r} - \mathbf{r}')^2 + 4d^2}} \quad (10)$$

is identical to the image charge potential (2) and is responsible for the localization. Based on the results of Eq. (8) we can establish the condition for an applicability of the image charge approach for the inducton problem. The extinction of the high k values in (8) resulting from the exponent e^{-kd} justifies the neglect of the term in the denominator for d larger than a few donor Bohr radii. For small d a deviation from the image charge potential should be expected for large k . The induced potential is slightly weaker than the one given by the image charge approach. The correction does not produce any qualitatively new effect for the inducton formation or its properties. However, it turns out that the imaginary part of potential (9) does. The imaginary part of (9) Fourier transformed into the real space yields a potential component which also can be expressed by the image charge potential

$$V_d^{Im}(\mathbf{r}, t) = -\frac{\hbar}{2\kappa k_F} \frac{\partial}{\partial t} U(\mathbf{r}, t). \quad (11)$$

For the inducton traveling as a stable wave packet with a constant velocity \mathbf{V} the charge density is given by $\rho_d^{el}(\mathbf{r}, t) = -|e|\psi_d(\mathbf{r} - \mathbf{V}t)^2$ and its Fourier transform by

$$\rho^{el}(k, \omega) = \int d^2r dt e^{i\mathbf{k}\cdot\mathbf{r} + i\omega t} \rho^{el}(\mathbf{r}, t) = 2\pi\delta(\omega - kV) \rho_d^{el}(k). \quad (12)$$

Then, the V_d^{Im} potential (11) depends on the inducton velocity and exerts on the inducton a force proportional to the value of the velocity but oriented opposite to its direction. We therefore expect a reduction of the inducton velocity and consequently dissipation of its kinetic energy. The dissipative potential (11) is inversely proportional to the Fermi wave vector k_F . In metal, due to the large value of the Fermi energy (eV) compared to the energy of the electron in a semiconductor quantum well (meV) the effect may not be observable. But, for the metal surface replaced by a two-dimensional electron gas, as discussed in the present model, the effect is likely to be experimentally resolvable.

IV. DUMPING OF THE INDUCTON MOTION

Let us assume a realistic (typical) structure for which such an experiment could be performed: a GaAs/Ga_xAl_{1-x}As layer heterostructure with the barrier height of 200 meV, and 2DEG formed of the electrons from the ionized donor centers embedded in the barrier. Then, the Fermi energy can at

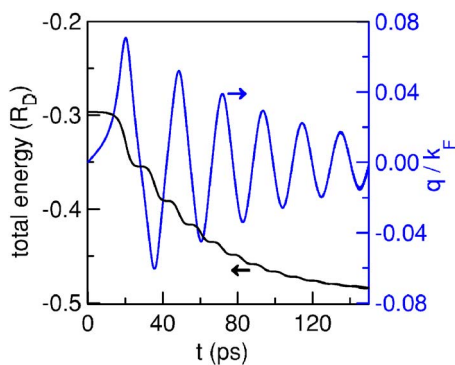


FIG. 2. (Color online) Total energy (left axis) and momentum normalized to the Fermi momentum (right axis) for the inducton oscillating inside a Gaussian potential cavity.

most reach the value of the barrier height. Therefore, let us assume $E_F=200$ meV, which gives $k_F=\sqrt{2mE_F}/\hbar=5.8a_D^{-1}$ ($a_D=\hbar^2\epsilon/m_e^2$ stands for the donor Bohr radius, for GaAs $a_D=9.8$ nm). We can calculate the surface density of the electron gas σ summing over the wave vectors inside the Fermi circle, $\sigma=k_F^2/2\pi=5.5\times 10^{12}$ cm $^{-2}$ [a typical value for 2DEG (Refs. 9 and 10)]. We will adopt a possibly small but realistic value of barrier width $d=1a_D$.

To illustrate the effect of the dissipative potential we form a standing ($\langle p \rangle = 0$) stationary inducton and then put it in motion multiplying the wave packet by a plane wave $\exp(iqx)$ for $q=0.1k_F$. V_d^{Im} and V_d^{Re} potentials are plotted in Fig. 1(b) with the solid and dashed lines, respectively. Note the energy scale differences for both the potentials. The inducton charge density is plotted with the dotted line. The “imaginary” component of the induced potential tends to stop the motion of the electron soliton. Figure 1(c) shows that due to the imaginary potential both the single electron and total energies decrease in time asymptotically to the values corresponding to the standing inducton. The momentum of the soliton decreases exponentially due to the dissipative force being proportional to the velocity.

Let us now consider the soliton motion inside a Gaussian potential cavity. The soliton oscillates inside the cavity (see Fig. 2) acquiring extremal momentum near the minimum of the confinement potential. The total inducton energy decreases monotonically. The steplike character of the curve is due to the increased dissipation rate when the inducton is moving the fastest. The time dependence of the momentum exhibits vanishing oscillations.

Potential (11) has an opposite sign to the time derivative of the image potential. It tends to resist against any potential changes, and hence against the change of the electron charge. In Fig. 3 we plotted the time dependence of the energy of a standing wave packet ($\langle p \rangle = 0$) which initially was not the

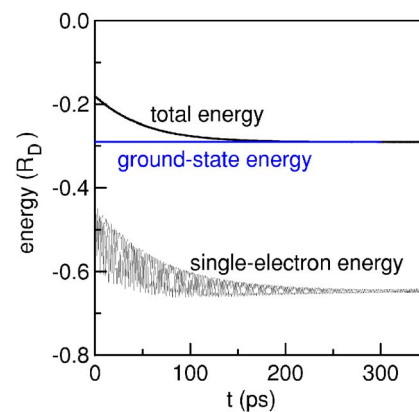


FIG. 3. (Color online) Total energy and single-electron energies for a standing nonstationary inducton relaxing to the stationary ground state.

eigenstate of the one-electron Hamiltonian. The charge density of such a wave packet oscillates, and the oscillations are visible in the time dependence of the single-electron energy. The dissipative part of the potential acts against these oscillations and eventually leads to their attenuation. On the other hand the total energy decreases monotonically to the ground-state eigenvalue. The excess energy is transferred to the electron gas forming an infinite energy reservoir kept at $T=0$ K.

V. SUMMARY

In conclusion, a single electron in a quantum well near a conducting surface or near a second quantum well containing a 2DEG induces a charge redistribution which results in a formation of the lateral confinement potential stabilizing the wave packet. The wave packet moves freely in the direction parallel to the conducting surface. Due to the nature of the stabilizing potential we called the wave packet an “inducton.” The inducton is characterized by two energies: the single-electron energy and the total energy. For an ideal conductor the total energy is conserved in the scattering processes. On the other hand the single-electron energy contains twice the interaction energy and exhibits oscillations during the scattering. We described the effect of the time-dependent part of the response of a realistic 2DEG on the inducton and explained that it contains a component of the potential tending to prevent any modification of the inducton charge distribution. This component leads to dissipation of the inducton kinetic energy, which is transferred to the electron gas. Similarly an inducton formed as a nonstationary wave packet relaxes to the stationary ground state.

ACKNOWLEDGMENT

This paper was supported by the Polish Government for Scientific Research (KBN) under Grant No. 1P03B 002 27.

- ¹P. Hawrylak, Phys. Rev. Lett. **71**, 3347 (1993).
- ²N. A. Bruce and P. A. Maksym, Phys. Rev. B **61**, 4718 (2000).
- ³S. Bednarek, B. Szafran, and J. Adamowski, Phys. Rev. B **61**, 4461 (2000).
- ⁴S. Bednarek, B. Szafran, and K. Lis, Phys. Rev. B **72**, 075319 (2005).
- ⁵M. Machado, E. V. Chulkov, V. M. Silkin, U. Hofer, and P. M. Echenique, Prog. Surf. Sci. **74**, 219 (2003); P. M. Echenique, F. Flores, and F. Sols, Phys. Rev. Lett. **55**, 2348 (1985).
- ⁶J. D. Fuhr, V. H. Ponce, F. J. Garcia de Abajo, and P. M. Echenique, Phys. Rev. B, **57**, 9329 (1998); A. Mazarro, P. M. Echenique, and R. H. Ritchie, *ibid.* **27**, 4117 (1983).
- ⁷M. Alducin, J. I. Juaristi, and P. M. Echenique, Surf. Sci. **559**, 233 (2004).
- ⁸T. Ando, A. B. Fowler, and F. Stern, Rev. Mod. Phys. **54**, 437 (1982).
- ⁹R. C. Ashoori, H. L. Stormer, J. S. Weiner, L. N. Pfeiffer, S. J. Pearton, K. W. Baldwin, and K. W. West, Phys. Rev. Lett. **68**, 3088 (1992).
- ¹⁰J. M. Elzerman, R. Hanson, L. H. Willems, L. M. K. Vandersypen, and L. P. Kouwenhoven, Appl. Phys. Lett. **84**, 4617 (2004).